# Single-Conductor Transmission Line Model Incorporating Radiation Reaction

Daiki Tashiro , *Member, IEEE*, Takashi Hisakado , *Member, IEEE*, Tohlu Matsushima , *Member, IEEE*, and Osami Wada , *Member, IEEE*

*Abstract*—**Increasing attention has been paid to the study of electromagnetic (EM) phenomena in complicated wire networks [e.g., metamaterials and EM compatibility (EMC)]. However, their lack of physical insights usually prevents systematic analysis of the phenomena. To address this, this article describes a transmission line (TL) model of a finite-length single conductor without a return current path to be applied as a fundamental physical model. The model includes radiation effects in a self-consistent way (i.e., its radiation reaction is included in an explicit way), and it is based on Sommerfeld principal wave propagation (strictly speaking, its behavior is asymptotic as the wire's conductivity approaches infinity). This formulation naturally leads to the consequence that the current flowing along a single conductor illuminated by an incident EM field is classified into three components, which are dominated by physically distinct principles, the principal wave itself ($I_{\mathrm{tr}}$, the traveling wave), the one reinduced by the traveling wave radiation ($I_{\mathrm{re}}$, the radiation reaction), and the one that directly scatters the incident field ($I_{\mathrm{sc}}$, the scattering wave). The EM energies of the traveling wave and radiation reaction components are stored in the TL and propagate, while the scattering component indicates an instantaneous scattering process. These components reveal the dynamical characteristics of a single-conductor TL model that includes radiation phenomena.**

*Index Terms*—**Common-mode current, radiation loss, single-conductor transmission line (TL), Sommerfeld wave, transmission line.**

## I. INTRODUCTION

CLASSICAL transmission line (TL) theory [1], [2] addresses the transmission of electromagnetic (EM) waves with specific modes that are characterized by the transverse shape and dimensions of the guiding structure. In recent years, however, an increasing number of cases that do not conform to the idealized telegrapher's equations have been assessed to account for the rising number of operating frequencies and the use of increasingly complicated three-dimensional wiring, as detailed in the introduction of [3]. Radiation losses and unintentional couplings become relatively large in such situations, where the actual phenomena deviate from the ideal case assumed in the classical model [4]. To overcome these difficulties, researchers investigating TL theory over the last few decades have exerted significant effort to broaden its scope of application to include non-TEM (nontransverse EM) phenomena, which were not included in the classical theory (e.g., [3], [5]–[10]).

The simple TL-like modeling of current propagation and radiation phenomena of a single conductor without a return current path is a fundamental and instructive pursuit and can also be used to model common-mode current. Furthermore, structures comprising multiple single-conductor lines have wide applicability in the study of metamaterials and plasmonics, with the goal of designing EM phenomena through the arrangement of objects, as in [11]–[13]. In a recent study on terahertz technology, a bare metal wire was experimentally shown to transmit waves with superior properties to those of a conventional waveguide [14], [15], in which such wires are expected to be formulated as TL elements.

A single conductor without a return current path serves as the basic weakly guiding component where radiation becomes predominant [16], [17]. From a simple observation of the phenomena that occur when the line is excited by an external EM field, two different principles appear to dominate; one is the instantaneous scattering, generating no dynamics unique to the structure by itself, and the other is wave propagation along the line, where the induced EM energies are temporarily stored in the structure and then reradiate through the process of multiple reflections. In fact, it is the latter component of these phenomena (i.e., the retardation caused by wave propagation) that plays a key role in TL dynamical properties, such as resonance and radiation losses. Therefore, the model that is designed to better understanding and gain insights regarding current propagation phenomena in a radiating TL should be highly detailed in terms of these phenomena. Furthermore, to elucidate the dynamic interaction between radiation and radiation-related losses in TLs, it is important (in the context as discussed in [18] and [19]) for the physical model to be self-consistent (e.g., it needs to observe the power conservation requirement by itself). This requires the explicit inclusion of radiation losses using the concept of "radiation reaction."

In a pioneering work by Sommerfeld, propagation of a surface wave along an infinite single conductor was theoretically

analyzed using cylindrical functions. He showed that the principal wave is guided along a wire of high, but not infinite, conductivity [20]. Subsequently, Goubau revealed that a single-conductor line coated by dielectrics adequately confines this wave [21].

In treating a finite-length single wire as a circuit element, the EM field radiation losses are significant, making it impossible to adopt the strict approach applied by Sommerfeld for an infinite wire. For example, [22] stated that the attenuation and distortion of the waveform of current flowing along a perfectly conducting single wire is inseparable from radiation phenomena. In this context, the manner in which the losses in TLs that counterbalance the field radiation is incorporated into a model becomes important. Although the governing equations of the generalized TL methods [3], [6] strictly follow the full-wave solution to Maxwell's equations with certain structural assumptions, they have difficulty in providing satisfactory explanations for consistent causality pertaining to radiation losses in the framework of TL theory (i.e., how radiation occurs, in what dynamical ways it contributes to losses, and how it is different from the ohmic losses). This is also the case for the methods presented in [23]–[25], which derive TL equations for a single conductor or the common-mode in multiconductor lines. The abovementioned approaches are sufficient for analysis, but they are not appropriate for design and synthesis of current flow in wiring structures.

This article presents a TL equation for current propagation along a thin and straight wire of perfect conductance without a return current path. The model is oriented for design and synthesis of EM phenomena, with clear descriptions of propagation along the line, radiation losses, and responses to external EM environments [26]. To integrate radiation losses in the TL dynamics of wave propagation along the line, it is rational to start with the principal wave, which is the only possible mode (independent of the external EM fields) in an infinite-length single conductor. For the case of a wire with finite length, radiation effects are explicitly incorporated into the model by the induction terms expressing the radiation reaction effect. This novel concept ensures self-consistency within the model, and elucidates the dynamical interaction of radiation losses, which is expected to enable analytical design of radiation phenomena in TLs. The model provides three components analytically classified as the traveling wave, the radiation reaction produced by the traveling wave, and the scattering component produced by an external excitation. These components reveal how structural discontinuities contribute to radiation in terms of field theory and to radiation losses in terms of circuit theory. They consistently explain the dynamics of a single-conductor TL, including radiation, allowing the model to be applicable to the design of EM phenomena around wiring structures with bends and branches.

## II. SINGLE-CONDUCTOR TL WITHOUT RADIATION REACTION

### A. Transmission Line Equation for the Sommerfeld Wave in an Infinite Single Conductor

In this section, we derive a homogeneous differential equation for the Sommerfeld principal wave in a thin wire with infinite
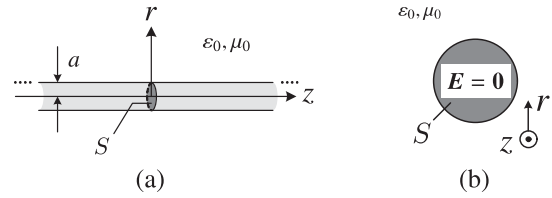


Fig. 1.    Infinitely long single-conductor line. (a) Side view. (b) Cross-sectional view.

length. The configuration of the system is displayed in Fig. 1, which shows an infinite wire with perfect conductance and radius $a$ oriented along the $z$-axis in free space. The factors $\varepsilon_0$ and $\mu_0$ are the permittivity and permeability in free space, respectively. In a sinusoidal steady state at an angular frequency of $\omega = 2\pi f$, the current density vector $\boldsymbol{J}$, and space charge density $\rho$ follow the charge conservation law

$$\boldsymbol{\nabla} \cdot \boldsymbol{J} + \mathrm{j}\omega\rho = 0. \tag{1}$$

Because it is assumed that the wire is sufficiently thin ($a \ll \lambda = 2\pi c/\omega$, where $c$ and $\lambda$ are the speed of light and the wavelength in free space, respectively), the thin-wire approximation is adopted to obtain the per unit length (p.u.l.) charge $Q(z)$ and current intensity $I(z)$ along the wire's axis by

$$Q(z) = \int_S \rho dS, \; I(z) = \int_S J_z dS \tag{2}$$

where $J_z$ is the $z$-directional component of $\boldsymbol{J}$ and $S$ is the cross-sectional area of the wire (see Fig. 1). Then, by integrating (1) over $S$ and applying (2), we obtain

$$\frac{dI(z)}{dz} + \mathrm{j}\omega Q(z) = 0. \tag{3}$$

The Maxwell equations for the electric field vector $\boldsymbol{E}$ in free space yield the wave equation of

$$\square^2 \boldsymbol{E} = -\frac{1}{\varepsilon_0}\boldsymbol{\nabla}\rho - \mathrm{j}\omega\mu_0\boldsymbol{J} \tag{4}$$

where $\square^2$ denotes the d'Alembert operator (defined by $\square^2 \equiv (\mathrm{j}\omega/c)^2 - \boldsymbol{\nabla}^2$ for a sinusoidal steady state at an angular frequency of $\omega$ [27]). The $z$-directional component of (4) is written as

$$\square^2 E_z = -\frac{1}{\varepsilon_0}\frac{d\rho}{dz} - \mathrm{j}\omega\mu_0 J_z. \tag{5}$$

Surface integration of (5) over the cross section $S$ using (2) yields

$$\square^2 \int_S E_z dS = -\frac{1}{\varepsilon_0}\frac{dQ(z)}{dz} - \mathrm{j}\omega\mu_0 I(z). \tag{6}$$

Specifically considering the principal wave without an exciting field, $E_z = 0$ inside the perfect conductor, and thus, we obtain

$$-\frac{1}{\varepsilon_0}\frac{dQ(z)}{dz} - \mathrm{j}\omega\mu_0 I(z) = 0. \tag{7}$$
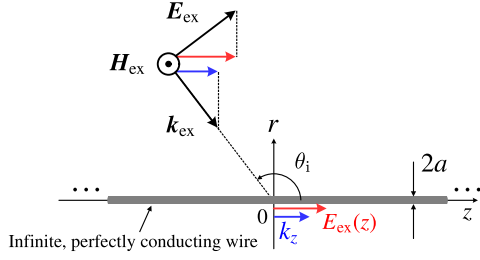
Fig. 2. EM field scattering by an infinite wire.

Combining (3) and (7) produces, for an infinitely long single conductor, a TL equation expressed as

$$\frac{d}{dz}\begin{bmatrix} cQ(z) \\ I(z) \end{bmatrix} = \begin{bmatrix} 0 & -\mathrm{j}k \\ -\mathrm{j}k & 0 \end{bmatrix}\begin{bmatrix} cQ(z) \\ I(z) \end{bmatrix} \qquad (8)$$

where $k \equiv \omega/c$. The solution to (8) corresponds to the asymptotic behavior of the Sommerfeld principal wave [20] traveling at the speed of light along a perfectly conducting wire.

### B. Formulation of External Excitation

Up to this point, we have considered current propagation along an infinite single conductor without external excitation. In this section, we formulate induction by an external field. Fig. 2 shows an infinitely long thin wire excited by a sinusoidal uniform plane wave with transverse magnetic polarization at an incident angle of $\theta_i$. In this case, $E_{\mathrm{ex}}$, the tangential component of the incident electric field vector $\boldsymbol{E}_{\mathrm{ex}}$, is periodic along the $z$-direction, as described by

$$E_{\mathrm{ex}}(z) = \hat{E}_{\mathrm{ex}}(k_z)\mathrm{e}^{-\mathrm{j}k_z z} \qquad (9)$$

where $k_z = -k\cos\theta_i$. The left-hand side of (6) should have a periodicity consistent with that of the incident electric field. As a result, (7) takes the form

$$-\frac{1}{\varepsilon_0}\frac{dQ(z)}{dz} - \mathrm{j}\omega\mu_0 I(z) = -\mathrm{j}\chi(k_z)\hat{E}_{\mathrm{ex}}(k_z)\mathrm{e}^{-\mathrm{j}k_z z} \qquad (10)$$

where $\chi(k_z)$ is a dimensionless factor of induction, the value of which will be determined later. Because (3), the charge conservation law, is also satisfied in the presence of an exciting field, the single-conductor TL equation under an exciting field becomes

$$\frac{d}{dz}\begin{bmatrix} cQ(z) \\ I(z) \end{bmatrix} = \begin{bmatrix} 0 & -\mathrm{j}k \\ -\mathrm{j}k & 0 \end{bmatrix}\begin{bmatrix} cQ(z) \\ I(z) \end{bmatrix}$$
$$+ \begin{bmatrix} \frac{\mathrm{j}\chi(k_z)}{Z_0}\hat{E}_{\mathrm{ex}}(k_z)\mathrm{e}^{-\mathrm{j}k_z z} \\ 0 \end{bmatrix} \qquad (11)$$

where $Z_0 = \sqrt{\mu_0/\varepsilon_0}$ is the characteristic impedance of free space.

Here, we briefly review the solutions to (11). Its homogeneous solution can be obtained by assuming $E_{\mathrm{ex}}(z) = 0$. This leads to

$$\begin{bmatrix} cQ_{\mathrm{tr}}(z) \\ I_{\mathrm{tr}}(z) \end{bmatrix} = I_f(0)\begin{bmatrix} 1 \\ 1 \end{bmatrix}\mathrm{e}^{-\mathrm{j}kz} + I_b(0)\begin{bmatrix} -1 \\ 1 \end{bmatrix}\mathrm{e}^{\mathrm{j}kz} \qquad (12)$$

which corresponds to the traveling wave of a single conductor. The two terms on the right-hand side of (12)

$$\begin{bmatrix} cQ_f(z) \\ I_f(z) \end{bmatrix} = I_f(0)\begin{bmatrix} 1 \\ 1 \end{bmatrix}\mathrm{e}^{-\mathrm{j}kz} \qquad (13)$$

$$\begin{bmatrix} cQ_b(z) \\ I_b(z) \end{bmatrix} = I_b(0)\begin{bmatrix} -1 \\ 1 \end{bmatrix}\mathrm{e}^{\mathrm{j}kz} \qquad (14)$$

correspond to the forward and backward waves, respectively. Equations (13) and (14) indicate that the p.u.l. charge and current of the traveling wave are constrained by the conditions $cQ_f = I_f$ and $cQ_b = -I_b$, and that they propagate at the speed of light along the wire.

For an incident electric field described by (9), the particular solution to (11) is periodic along the line

$$\begin{bmatrix} cQ_{\mathrm{sc}}(z) \\ I_{\mathrm{sc}}(z) \end{bmatrix} = \frac{\chi(k_z)}{(k^2 - k_z^2)Z_0}\begin{bmatrix} k_z \\ k \end{bmatrix}\hat{E}_{\mathrm{ex}}(k_z)\mathrm{e}^{-\mathrm{j}k_z z}. \qquad (15)$$

The Fourier coefficient for this equation is

$$\begin{bmatrix} c\hat{Q}_{\mathrm{sc}}(k_z) \\ \hat{I}_{\mathrm{sc}}(k_z) \end{bmatrix} = \frac{\chi(k_z)}{(k^2 - k_z^2)Z_0}\begin{bmatrix} k_z \\ k \end{bmatrix}\hat{E}_{\mathrm{ex}}(k_z) \qquad (16)$$

which corresponds to the source of the EM field scattering for a $z$-directional angular wave number $k_z$ on the surface of the wire.

The coefficient $\chi(k_z)$ is then fixed by comparing (16) to the solution of the EM field scattering problem for an infinite-length thin wire. For the configuration shown in Fig. 2, the tangential component of the scattered electric field and the current on the surface can be obtained with EM field scattering theory [28], [29] using a thin-wire approximation that considers only the axisymmetric mode, as described by

$$E_{\mathrm{ex}}(z) = \left(k^2 - k_z^2\right)A\mathrm{e}^{-\mathrm{j}k_z z}J_0\left(a\sqrt{k^2 - k_z^2}\right) \qquad (17)$$

and

$$I_{\mathrm{sc}}(z) = \frac{4kA\mathrm{e}^{-\mathrm{j}k_z z}}{Z_0 H_0^{(2)}\left(a\sqrt{k^2 - k_z^2}\right)} \qquad (18)$$

where $A$ denotes the amplitude consistently used in (17) and (18), $J_0$ is the Bessel function of zeroth order and first kind, and $H_0^{(2)}$ is the Hankel function of zeroth order and second kind. Equations (17) and (18) yield the following relation between $I_{\mathrm{sc}}$ and $E_{\mathrm{ex}}$

$$I_{\mathrm{sc}}(z) = \frac{4kE_{\mathrm{ex}}(z)}{(k^2 - k_z^2)Z_0 J_0\left(a\sqrt{k^2 - k_z^2}\right)H_0^{(2)}\left(a\sqrt{k^2 - k_z^2}\right)}. \qquad (19)$$

By comparing (19) to the current obtained in (16) within the range $|k_z| < k$, the factor $\chi(k_z)$ is determined by

$$\chi(k_z) = \frac{4}{J_0\left(a\sqrt{k^2 - k_z^2}\right)H_0^{(2)}\left(a\sqrt{k^2 - k_z^2}\right)}. \qquad (20)$$

For the condition $k < |k_z|$, in which the field is evanescent and the corresponding scattering problem is not assumed to represent

TABLE I
CORRESPONDENCE OF TL PARAMETERS

| | Two-wire TL | Single-conductor TL |
|---|---|---|
| Equation | Eq. (24) | Eq. (23) |
| Variables | $V(z)$, $I(z)$ | $cQ(z)$, $I(z)$ |
| Ratio of variables of each mode | $\pm\sqrt{\frac{L}{C}}$ | $\pm 1$ |
| Phase constant | $\omega\sqrt{LC}$ | $\frac{\omega}{c} = k$ |

an actual phenomenon, the coefficient must be determined to enable the formulation of a TL equation for the finite-length line (described in Section III). With an extension of the Bessel functions (see, e.g., [30]), it becomes

$$\chi(k_z) = \frac{-2\pi j}{I_0\left(a\sqrt{k_z^2 - k^2}\right) K_0\left(a\sqrt{k_z^2 - k^2}\right)} \quad (21)$$

where $I_0$ and $K_0$ are the modified Bessel functions of zeroth order and first and second kind, respectively.

Equation (11) corresponds to an exciting field with a single angular wave number, $k_z$. For an incident field $E_{\text{ex}}(z)$ with the wave components

$$E_{\text{ex}}(z) = \sum_m \hat{E}_{\text{ex}}(k_m) e^{-jk_m z} \quad (22)$$

where $m$ is an index number, $\chi(k_m)$ is determined for each $k_m$ by (20) and (21), and the single-conductor TL equation becomes

$$\frac{d}{dz}\begin{bmatrix} cQ(z) \\ I(z) \end{bmatrix} = \begin{bmatrix} 0 & -jk \\ -jk & 0 \end{bmatrix}\begin{bmatrix} cQ(z) \\ I(z) \end{bmatrix} + \begin{bmatrix} \sum_m \frac{j\chi(k_m)}{Z_0} \hat{E}_{\text{ex}}(k_m) e^{-jk_m z} \\ 0 \end{bmatrix} \quad (23)$$

for a generalized expression of (11). The inhomogeneous term indicates that this equation treats the induction by the external EM field as a distributed source excitation.

### C. Correspondence to the Two-Wire TL Equation

In this section, the proposed (23) is compared to the two-wire TL equation with a distributed voltage source $V_f(z)$ and current source $I_f(z)$ (introduced in, e.g., [1], [31])

$$\frac{d}{dz}\begin{bmatrix} V(z) \\ I(z) \end{bmatrix} = \begin{bmatrix} 0 & -j\omega L \\ -j\omega C & 0 \end{bmatrix}\begin{bmatrix} V(z) \\ I(z) \end{bmatrix} - \begin{bmatrix} V_f(z) \\ I_f(z) \end{bmatrix} \quad (24)$$

where $V$ and $I$ are the line voltages and currents, respectively, and $L$ and $C$ are the p.u.l. inductance and capacitance, respectively. The TL parameters produced by the corresponding equations are listed in Table I. The important parameters in the two-wire TL equation are the characteristic impedance (given by the ratio of the variables for each propagation mode, $V_*/I_*$, where $*$ determines whether the wave is forward- or backward-traveling) and a phase constant ($\omega\sqrt{LC}$ for a lossless line). Similarly, the single-conductor TL equation uses $cQ(z)$ and $I(z)$ as variables to obtain a normalized expression for each mode in terms of their ratio, $\pm 1$ [see (12)], and the phase constant $\omega/c = k$. Unlike the approaches in [23] and [25], these circuit constants are independent of the position along the wire,
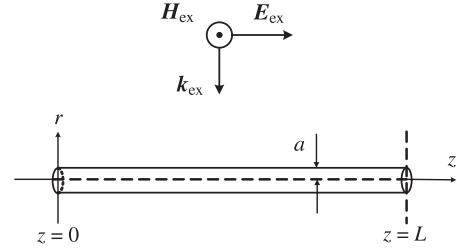


Fig. 3. Finite-length single-conductor line excited by a sinusoidal plane wave.

$z$, because the proposed equation is based on the dynamics of the principal wave. Based on this correspondence, the proposed single-wire model can be treated in a manner analogous to two-wire TL theory.

### D. Example Without Radiation Loss Considered

In this section, we test a preliminary version of a model without the finite-length effect and radiation reaction factors needed to describe a finite-length wire (these are introduced in Sections III and IV, respectively). The configuration of the intermediate model is presented in Fig. 3, which shows a line of length $L$ excited by an in-phase uniform sinusoidal plane wave

$$E_{\text{ex}}(z) = E_0 \ (\text{constant}). \quad (25)$$

Based on these conditions, the current amplitude at the center position ($z = \frac{L}{2}$) is calculated. The total distribution can be obtained by the superposition of the traveling wave in (12) and the source of the scattered wave derived by substituting (25) into (15)

$$\begin{bmatrix} cQ_{\text{sc}}(z) \\ I_{\text{sc}}(z) \end{bmatrix} = \begin{bmatrix} 0 \\ \frac{\chi(0)E_0}{kZ_0} \end{bmatrix}. \quad (26)$$

As the two terminals are open-circuited (not connected to another single-conductor line), Kirchhoff's current law (KCL) yields

$$I_{\text{tr}}(0) + I_{\text{sc}}(0) = 0 \quad (27)$$

$$I_{\text{tr}}(L) + I_{\text{sc}}(L) = 0. \quad (28)$$

The traveling and scattering components are completely independent in the case of a line with infinite length, but here Kirchhoff's law is applied to solve for a line with finite length. These can be rewritten using $I_f(0)$ and $I_b(L)$ as

$$\begin{bmatrix} 1 & e^{-jkL} \\ e^{-jkL} & 1 \end{bmatrix}\begin{bmatrix} I_f(0) \\ I_b(L) \end{bmatrix} = \begin{bmatrix} -I_{\text{sc}}(0) \\ -I_{\text{sc}}(L) \end{bmatrix}. \quad (29)$$

Here, (23) is reduced to simultaneous linear equations to obtain the terminal values of the traveling wave. Equation (29) can then be solved for all cases with the exception of $\sin kL = 0$ (corresponding to the resonant and antiresonant frequencies), and the total values can be obtained from (13), (14), and (26) as

$$\begin{bmatrix} cQ(z) \\ I(z) \end{bmatrix} = \frac{(e^{jkL} - 1)\, j\chi(0)E_0}{2kZ_0 \sin kL}\begin{bmatrix} 1 \\ 1 \end{bmatrix} e^{-jkz}$$
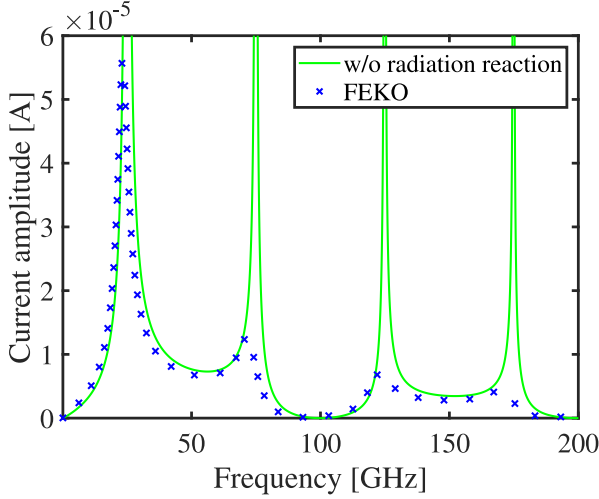
Fig. 4.   Frequency characteristics of current amplitude at the center of a wire ($L = 6$ mm, $a = 15$ $\mu$m) excited by a plane wave ($E_0 = 1$ V/m). Because radiation losses are not included here, the current at $z = \frac{L}{2}$ diverges at resonant frequencies.

$$- \frac{\left(\mathrm{e}^{-\mathrm{j}kL} - 1\right) \mathrm{j}\chi(0)E_0}{2kZ_0 \sin kL} \begin{bmatrix} -1 \\ 1 \end{bmatrix} \mathrm{e}^{\mathrm{j}kz}$$

$$+ \begin{bmatrix} 0 \\ \frac{\chi(0)E_0}{kZ_0} \end{bmatrix}. \qquad (30)$$

As with the case of the infinite wire (but with KCL imposed by applying a finite length $L$), the variables expressed in (30) correspond to a traveling wave and a scattering source with a wave number corresponding to that of the incident field (for which $z$ is constant). Substituting $z = \frac{L}{2}$ into the second row of (30), the current at the center of the wire becomes

$$I\left(\frac{L}{2}\right) = \frac{\left(\mathrm{e}^{\mathrm{j}kL} - 1\right) \mathrm{j}\chi(0)E_0}{2kZ_0 \sin kL} \mathrm{e}^{-\mathrm{j}k\frac{L}{2}}$$

$$- \frac{\left(\mathrm{e}^{-\mathrm{j}kL} - 1\right) \mathrm{j}\chi(0)E_0}{2kZ_0 \sin kL} \mathrm{e}^{\mathrm{j}k\frac{L}{2}}$$

$$+ \frac{\chi(0)E_0}{kZ_0}. \qquad (31)$$

Fig. 4 shows the frequency characteristics of the current amplitude of (31) for $L = 6$ mm, $a = 15$ $\mu$m, and $E_0 = 1$ V/m. The result was compared to a numerical solution obtained by applying the method of moments (MoM) through the FEKO software package. The characteristics were found to be in general agreement, although the current amplitude diverged at the resonant frequencies because (29) degenerates at $\sin kL = 0$, as it does not consider radiation losses for a finite-length wire. This factor becomes particularly essential at resonant frequencies, at which there are large amounts of radiation losses as a result of the size of the propagating wave.

Thus, it is necessary for the radiation losses to be included in the extension of the proposed TL equation for the case of a finite-length wire. To achieve full modeling of a single-conductor TL with finite length, Section III extends the scattering problem

to a finite-length wire and Section IV introduces the radiation reaction as a feedback effect of the traveling wave radiation.

### III.   EXTENSION OF PARTICULAR SOLUTION TO A SINGLE CONDUCTOR OF FINITE LENGTH

#### A.   Particular Solution With a Finite-Length Effect

As (23) is derived for an infinite wire, extending it to the modeling of a finite-length single conductor requires the addition of correction terms to the external field $E_{\mathrm{ex}}$ to obtain a complete exciting field. In this section, this supplementary field is formulated and the solution for a finite-length wire, which corresponds to (16) in the limiting case of an infinite wire, is derived.

We preliminarily express an external electric field $E_{\mathrm{ex}}$ incident on a finite-length wire in terms of the Fourier series described by

$$E_{\mathrm{ex}}(z) = \sum_{m=-M}^{M} \hat{E}_{\mathrm{ex}}(k_m)\mathrm{e}^{-\mathrm{j}k_m z} \qquad (32)$$

$$\hat{E}_{\mathrm{ex}}(k_m) = \frac{1}{L} \int_0^L E_{\mathrm{ex}}(z)\mathrm{e}^{\mathrm{j}k_m z} dz \qquad (33)$$

$$k_m = \frac{2\pi m}{L} \quad (m = -M, \ldots, M) \qquad (34)$$

where $M$ is an integer that approximates the field $E_{\mathrm{ex}}(z)$. From (16), the components of the p.u.l. charge $c\hat{Q}_{\mathrm{sc}}(k_n)$ and current $\hat{I}_{\mathrm{sc}}(k_n)$ at angular wave number $k_n$ are constrained by

$$c\hat{Q}_{\mathrm{sc}}(k_n) = \frac{k_n}{k} \hat{I}_{\mathrm{sc}}(k_n). \qquad (35)$$

In the formulation in Section II, the scattered field in the range $z = (-\infty, 0], [L, \infty)$ was taken into consideration, and it is now subtracted through what is referred to in this article as a "finite-length effect." The subtracted field $E_n^{(\mathrm{sc})}$ for a scattering source with angular wave number $k_n$ is expressed as

$$E_n^{(\mathrm{sc})} = - \frac{d\phi}{dz} - \mathrm{j}\omega A_z$$

$$= - \frac{1}{\varepsilon_0} \left(\int_{-\infty}^0 + \int_L^\infty\right) \frac{dG(z-\xi, a)}{dz} \hat{Q}_{\mathrm{sc}}(k_n)\mathrm{e}^{-\mathrm{j}k_n\xi} d\xi$$

$$- \mathrm{j}\omega\mu_0 \left(\int_{-\infty}^0 + \int_L^\infty\right) G(z-\xi, a)\hat{I}_{\mathrm{sc}}(k_n)\mathrm{e}^{-\mathrm{j}k_n\xi} d\xi$$

$$= - \frac{1}{\varepsilon_0} \left(\int_{-\infty}^\infty - \int_0^L\right) \frac{dG(z-\xi, a)}{dz} \hat{Q}_{\mathrm{sc}}(k_n)\mathrm{e}^{-\mathrm{j}k_n\xi} d\xi$$

$$- \mathrm{j}\omega\mu_0 \left(\int_{-\infty}^\infty - \int_0^L\right) G(z-\xi, a)\hat{I}_{\mathrm{sc}}(k_n)\mathrm{e}^{-\mathrm{j}k_n\xi} d\xi$$

$$\qquad (36)$$

where $\phi$ and $A_z$ are the Lorenz gauge potentials and

$$G(z, r) = \frac{\mathrm{e}^{-\mathrm{j}k\sqrt{z^2+r^2}}}{4\pi\sqrt{z^2+r^2}} \qquad (37)$$

is the retarded Green's function. Because the external and supplementary fields $E_{\mathrm{ex}}$ and $E_n^{(\mathrm{sc})}$, respectively, induce scattering sources, the particular solution for the evaluated angular wave number $k_m$ is obtained as an extension of (16)

$$\begin{bmatrix} c\hat{Q}_{\mathrm{sc}}(k_m) \\ \hat{I}_{\mathrm{sc}}(k_m) \end{bmatrix} = \frac{\chi(k_m)}{(k^2 - k_m^2)Z_0} \begin{bmatrix} k_m \\ k \end{bmatrix} \left\{ \hat{E}_{\mathrm{ex}}(k_m) - \sum_{n=-M}^{M} \hat{E}_n^{(\mathrm{sc})}(k_m) \right\}. \tag{38}$$

### B. Analytical Expressions of the Scattering Sources

In the corrected particular solution expressed by (38), the scattering current $\hat{I}_{\mathrm{sc}}(k_m)$ remains in $\hat{E}_n^{(\mathrm{sc})}(k_m)$ on the right-hand side, just as in (36). As a result, (38) is not truly solved for $\hat{I}_{\mathrm{sc}}(k_m)$. To obtain an analytical solution, it is necessary to find a method for addressing the infinite integration in (36). As expressed by (36), the electric field $E_n^{(\mathrm{sc})}$ can be separated into two intervals: $(-\infty, \infty)$ and $[0, L]$. Because the phase of the scattered field opposes that of the incident field when evaluated along the wire's surface, the infinite integration component from the scattering problem for an infinite wire can be replaced analytically by

$$-\frac{1}{\varepsilon_0} \int_{-\infty}^{\infty} \frac{dG(z-\xi,\, a)}{dz} \hat{Q}_{\mathrm{sc}}(k_n) e^{-jk_n\xi} d\xi$$

$$-j\omega\mu_0 \int_{-\infty}^{\infty} G(z-\xi,\, a) \hat{I}_{\mathrm{sc}}(k_n) e^{-jk_n\xi} d\xi$$

$$= -\frac{(k^2 - k_n^2)Z_0}{k\chi(k_n)} e^{-jk_n z} \hat{I}_{\mathrm{sc}}(k_n). \tag{39}$$

Therefore, by expressing the Fourier component of (36) as

$$\hat{E}_n^{(\mathrm{sc})}(k_m) = \hat{Z}_n(k_m) \hat{I}_{\mathrm{sc}}(k_n) \tag{40}$$

the coefficient $\hat{Z}_n(k_m)$ becomes

$$\hat{Z}_n(k_m) \equiv -\frac{(k^2 - k_n^2)Z_0}{k\chi(k_n)} \delta_{mn} + \hat{Z}_n'(k_m) \tag{41}$$

$$\hat{Z}_n'(k_m) \equiv -\frac{(k^2 - k_m k_n)Z_0}{jk}.$$

$$\frac{1}{L} \int_0^L \int_0^L e^{-jk_n\xi} G(z-\xi,\, a) d\xi e^{jk_m z} dz \tag{42}$$

where $\delta_{mn}$ denotes the Kronecker delta. The first term on the right-hand side of (41) is nonzero only when $n = m$, which cancels the left-hand side in (38), yielding

$$\hat{E}_{\mathrm{ex}}(k_m) - \sum_{n=-M}^{M} \hat{Z}_n'(k_m) \hat{I}_{\mathrm{sc}}(k_n) = 0 \tag{43}$$

for each $m = -M, \ldots, M$. By defining the vectors and the coefficient matrix as

$$\hat{\boldsymbol{I}}_{\mathrm{sc}} \equiv \begin{bmatrix} \hat{I}_{\mathrm{sc}}(k_{-M}) \\ \vdots \\ \hat{I}_{\mathrm{sc}}(k_M) \end{bmatrix} \tag{44}$$

$$\hat{\boldsymbol{Z}}' \equiv \begin{bmatrix} \hat{Z}_{-M}'(k_{-M}) & \ldots & \hat{Z}_M'(k_{-M}) \\ \vdots & \ddots & \vdots \\ \hat{Z}_{-M}'(k_M) & \ldots & \hat{Z}_M'(k_M) \end{bmatrix} \tag{45}$$

$$\hat{\boldsymbol{E}}_{\mathrm{ex}} \equiv \begin{bmatrix} \hat{E}_{\mathrm{ex}}(k_{-M}) \\ \vdots \\ \hat{E}_{\mathrm{ex}}(k_M) \end{bmatrix} \tag{46}$$

the current vector $\hat{\boldsymbol{I}}_{\mathrm{sc}}$ can be obtained from (43) as

$$\hat{\boldsymbol{I}}_{\mathrm{sc}} = \hat{\boldsymbol{Z}}'^{-1} \hat{\boldsymbol{E}}_{\mathrm{ex}} \tag{47}$$

which describes the scattering current and includes the finite-length effect. As $c\hat{Q}_{\mathrm{sc}}(k_m)$ and $\hat{I}_{\mathrm{sc}}(k_m)$ are under the constraint of (35), this can be expressed as

$$c\hat{\boldsymbol{Q}}_{\mathrm{sc}} = \boldsymbol{W}\hat{\boldsymbol{I}}_{\mathrm{sc}} \tag{48}$$

$$\boldsymbol{W} = \mathrm{diag}\left(\frac{k_{-M}}{k},\, \ldots,\, \frac{k_M}{k}\right) \tag{49}$$

where $\mathrm{diag}()$ denotes the diagonal matrix. From (47) and (48), the scattering p.u.l. charge can be obtained as

$$c\hat{\boldsymbol{Q}}_{\mathrm{sc}} = \boldsymbol{W}\hat{\boldsymbol{Z}}'^{-1} \hat{\boldsymbol{E}}_{\mathrm{ex}}. \tag{50}$$

Defining the inverse discrete Fourier transform operation $\mathcal{F}^{-1}[\cdot]$ as

$$I_{\mathrm{sc}}(z) = \mathcal{F}^{-1}[\hat{\boldsymbol{I}}_{\mathrm{sc}}] = \sum_m \hat{I}_{\mathrm{sc}}(k_m) e^{-jk_m z} \tag{51}$$

from (47) and (50), we obtain

$$I_{\mathrm{sc}}(z) = \mathcal{F}^{-1}\left[\hat{\boldsymbol{Z}}'^{-1} \hat{\boldsymbol{E}}_{\mathrm{ex}}\right] \tag{52}$$

$$cQ_{\mathrm{sc}}(z) = \mathcal{F}^{-1}\left[\boldsymbol{W}\hat{\boldsymbol{Z}}'^{-1} \hat{\boldsymbol{E}}_{\mathrm{ex}}\right] \tag{53}$$

which have a form to which the boundary condition (KCL) given in Section V applies.

### IV. RADIATION AND INDUCED REACTION BY TRAVELING WAVE ELEMENT

In the preceding section, (38) was used to extend the EM field scattering problem to a finite-length wire. In this section, the effect of the radiation emitted by a traveling wave element is formulated to introduce the radiation reaction effect to the finite-length model. In addition, we obtain the induced p.u.l. charge and current components as radiation reaction terms.

As noted in Section II, the electric field emitted by a traveling wave will have no $z$-directional component as long as the wave keeps propagating along an infinite line. For the finite-length wire case, however, this component will become nonzero [32].

This nonzero component, which induces a current with retardation in the wire itself, results in losses in terms of the TL performance.

As discussed in [33], the $z$-directional component of an electric field emitted by a traveling wave element can be expressed simply. The electric field generated by the propagation of the forward wave in (13) from $z = 0$ to $z = L$ along the wire, as observed at point $P(z, r)$, becomes

$$
\begin{aligned}
E_z^f(z, r) &= Z_0 \left\{ -G(z, r)I_f(0) + G(z - L, r)I_f(L) \right\} \\
&= Z_0 \left\{ -G(z, r) + G(z - L, r)e^{-jkL} \right\} I_f(0)
\end{aligned}
\tag{54}
$$

whereas that induced by the backward wave in (14) as it propagates from $z = L$ to $z = 0$ is given by

$$
\begin{aligned}
E_z^b(z, r) &= Z_0 \left\{ G(z, r)I_b(0) - G(z - L, r)I_b(L) \right\} \\
&= Z_0 \left\{ G(z, r)e^{-jkL} - G(z - L, r) \right\} I_b(L).
\end{aligned}
\tag{55}
$$

$E_f(z)$, the electric field in (54) evaluated at the surface of the wire ($r = a$), then becomes

$$
E_f(z) = Z_0 \left\{ -G_0(z) + G_L(z)e^{-jkL} \right\} I_f(0)
\tag{56}
$$

whereas, from (55), the backward wave induces a field $E_b(z)$ given by

$$
E_b(z) = Z_0 \left\{ G_0(z)e^{-jkL} - G_L(z) \right\} I_b(L).
\tag{57}
$$

Here, $G_0(z)$ and $G_L(z)$ are one-dimensional expressions of Green's function evaluated at the surface point $(z, r) = (z, a)$ from the respective wire terminals $(z, r) = (0, 0)$, $(L, 0)$, as defined by (37)

$$
G_0(z) \equiv G(z, a)
\tag{58}
$$

$$
G_L(z) \equiv G(z - L, a).
\tag{59}
$$

The Fourier coefficients of (56) and (57), $\hat{E}_f$ and $\hat{E}_b$, respectively, become

$$
\hat{E}_f(k_m) = \hat{Z}_f(k_m)I_f(0)
\tag{60}
$$

$$
\hat{E}_b(k_m) = \hat{Z}_b(k_m)I_b(L)
\tag{61}
$$

where

$$
\hat{Z}_f(k_m) \equiv Z_0 \left\{ -\hat{G}_0(k_m) + \hat{G}_L(k_m)e^{-jkL} \right\}
\tag{62}
$$

$$
\hat{Z}_b(k_m) \equiv Z_0 \left\{ \hat{G}_0(k_m)e^{-jkL} - \hat{G}_L(k_m) \right\}.
\tag{63}
$$

Then, defining the $k$-space sampling vectors as

$$
\hat{\boldsymbol{E}}_f \equiv
\begin{bmatrix}
\hat{E}_f(k_{-M}) \\
\vdots \\
\hat{E}_f(k_M)
\end{bmatrix}, \quad
\hat{\boldsymbol{E}}_b \equiv
\begin{bmatrix}
\hat{E}_b(k_{-M}) \\
\vdots \\
\hat{E}_b(k_M)
\end{bmatrix}
\tag{64}
$$

and

$$
\hat{\boldsymbol{Z}}_f \equiv
\begin{bmatrix}
\hat{Z}_f(k_{-M}) \\
\vdots \\
\hat{Z}_f(k_M)
\end{bmatrix}, \quad
\hat{\boldsymbol{Z}}_b \equiv
\begin{bmatrix}
\hat{Z}_b(k_{-M}) \\
\vdots \\
\hat{Z}_b(k_M)
\end{bmatrix}
\tag{65}
$$

the current induced in the wire as a reaction effect against the field radiation produced by the traveling wave

$$
\hat{\boldsymbol{I}}_{\mathrm{re}}^{(f)} \equiv
\begin{bmatrix}
\hat{I}_{\mathrm{re}}^{(f)}(k_{-M}) \\
\vdots \\
\hat{I}_{\mathrm{re}}^{(f)}(k_M)
\end{bmatrix}, \quad
\hat{\boldsymbol{I}}_{\mathrm{re}}^{(b)} \equiv
\begin{bmatrix}
\hat{I}_{\mathrm{re}}^{(b)}(k_{-M}) \\
\vdots \\
\hat{I}_{\mathrm{re}}^{(b)}(k_M)
\end{bmatrix}
\tag{66}
$$

can be obtained by applying the same process through which (47) was derived in Section III

$$
\hat{\boldsymbol{I}}_{\mathrm{re}}^{(f)} = \hat{\boldsymbol{Z}}'^{-1} \hat{\boldsymbol{E}}_z^f = \hat{\boldsymbol{Z}}'^{-1} \hat{\boldsymbol{Z}}_f I_f(0)
\tag{67}
$$

$$
\hat{\boldsymbol{I}}_{\mathrm{re}}^{(b)} = \hat{\boldsymbol{Z}}'^{-1} \hat{\boldsymbol{E}}_z^b = \hat{\boldsymbol{Z}}'^{-1} \hat{\boldsymbol{Z}}_b I_b(L).
\tag{68}
$$

Equations (67) and (68) express the reaction currents induced by the radiation that is produced by the traveling waves. In deriving these equations, the finite-length effect must be considered as an induction effect, which renders its electric fields, $\hat{E}_n^{(f)}$ and $\hat{E}_n^{(b)}$, as

$$
\hat{E}_n^{(f)}(k_m) = \hat{Z}_n(k_m)\hat{I}_{\mathrm{re}}^{(f)}(k_n)
\tag{69}
$$

$$
\hat{E}_n^{(b)}(k_m) = \hat{Z}_n(k_m)\hat{I}_{\mathrm{re}}^{(b)}(k_n).
\tag{70}
$$

The distributions of the reaction currents along the TL are obtained by applying inverse transformations of (67) and (68) to obtain

$$
I_{\mathrm{re}}^{(f)}(z) = \alpha_{\mathrm{re}}^{(f)}(z)I_f(0)
\tag{71}
$$

$$
I_{\mathrm{re}}^{(b)}(z) = \alpha_{\mathrm{re}}^{(b)}(z)I_b(L)
\tag{72}
$$

where $\alpha_{\mathrm{re}}^{(f)}(z)$ and $\alpha_{\mathrm{re}}^{(b)}(z)$ are derived from (67) and (68), respectively, as

$$
\alpha_{\mathrm{re}}^{(f)}(z) = \mathcal{F}^{-1}\left[ \hat{\boldsymbol{Z}}'^{-1} \hat{\boldsymbol{Z}}_f \right]
\tag{73}
$$

$$
\alpha_{\mathrm{re}}^{(b)}(z) = \mathcal{F}^{-1}\left[ \hat{\boldsymbol{Z}}'^{-1} \hat{\boldsymbol{Z}}_b \right].
\tag{74}
$$

The distributions of linear charge density produced by the radiation reaction can be derived as

$$
cQ_{\mathrm{re}}^{(f)}(z) = \zeta_{\mathrm{re}}^{(f)}(z)I_f(0)
\tag{75}
$$

$$
cQ_{\mathrm{re}}^{(b)}(z) = \zeta_{\mathrm{re}}^{(b)}(z)I_b(L)
\tag{76}
$$

where

$$
\zeta_{\mathrm{re}}^{(f)}(z) = \mathcal{F}^{-1}\left[ \boldsymbol{W} \hat{\boldsymbol{Z}}'^{-1} \hat{\boldsymbol{Z}}_f \right]
\tag{77}
$$

$$
\zeta_{\mathrm{re}}^{(b)}(z) = \mathcal{F}^{-1}\left[ \boldsymbol{W} \hat{\boldsymbol{Z}}'^{-1} \hat{\boldsymbol{Z}}_b \right].
\tag{78}
$$

For simplicity, the sum of the reaction currents and line charges of the forward and backward waves can be expressed as $I_{\mathrm{re}} \equiv I_{\mathrm{re}}^{(f)} + I_{\mathrm{re}}^{(b)}$ and $cQ_{\mathrm{re}} \equiv cQ_{\mathrm{re}}^{(f)} + cQ_{\mathrm{re}}^{(b)}$, respectively.

## V. SINGLE-CONDUCTOR TL EQUATION AND APPLICATION OF KCL AT THE TERMINALS

By combining the finite-length effect (see Section III) and the reaction effect produced by the radiation that is induced by the traveling wave element (see Section IV), a single-conductor
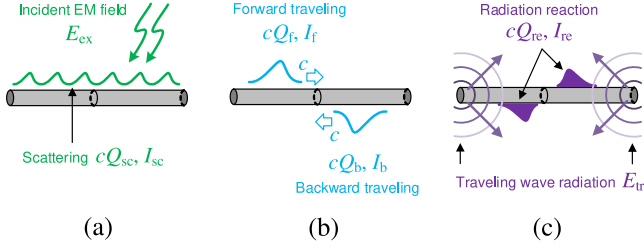
Fig. 5. Three physical components in the presented single-conductor TL theory. These components comprise a totally self-consistent model, with each reflecting physically distinct principles. (a) Scattering. (b) Traveling. (c) Reaction.
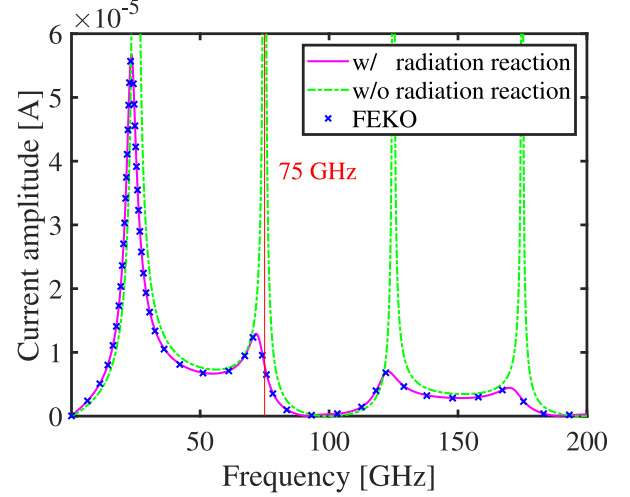


Fig. 6. Evaluation of radiation reaction for the conditions shown in Fig. 4. The radiation reaction suppresses the divergence of the current amplitude at resonant frequencies, yielding good agreement with the calculation obtained by MoM.

TL equation for a finite-length wire, which describes the physical components shown in Fig. 5 can be formulated. The first component is the scattering source distribution described in Fig. 5(a), and it is described by (79) shown at the bottom of this page, with the excitation by the external field [see (32)] along with its finite-length effect [see (40)]. Fig. 5(b) shows the free propagation of the traveling wave, which serves as the most basic of dynamics in a single-conductor line governed by the wave equation [see (8)]. The radiation reaction component in Fig. 5(c) is important for self-consistent modeling. Its TL equations for the forward and backward traveling waves are (80) and (81) shown at the bottom of this page, respectively. The reaction component arises with the excitation of retarded electric fields [see (56) and (57)] induced in the wire by the traveling wave element, with their respective finite-length effects [see (69) and (70)] included.

As expressed here, these equations contain some of the forcing term variables as feedback effects. In each equation, the second term on the right-hand side indicates induction by the external field, as given in (79), and by the reaction field, as given in (80) and (81). The third term in each equation relates to the finite-length effect.

The total linear charge density $cQ$ and current $I$ can then be derived as superpositions of the traveling wave, radiation reaction, and scattered field source as

$$cQ(z) = c \{ Q_{\text{tr}}(z) + Q_{\text{re}}(z) + Q_{\text{sc}}(z) \} \tag{82}$$

$$I(z) = I_{\text{tr}}(z) + I_{\text{re}}(z) + I_{\text{sc}}(z). \tag{83}$$

$$\frac{d}{dz} \begin{bmatrix} cQ_{\text{sc}} \\ I_{\text{sc}} \end{bmatrix} = \begin{bmatrix} 0 & -jk \\ -jk & 0 \end{bmatrix} \begin{bmatrix} cQ_{\text{sc}} \\ I_{\text{sc}} \end{bmatrix} + \begin{bmatrix} \displaystyle\sum_m \frac{j\chi(k_m)}{Z_0} \hat{E}_{\text{ex}}(k_m) e^{-jk_m z} \\ 0 \end{bmatrix} - \begin{bmatrix} \displaystyle\sum_m \frac{j\chi(k_m)}{Z_0} \sum_n \hat{Z}_n(k_m) \hat{I}_{\text{sc}}(k_n) e^{-jk_m z} \\ 0 \end{bmatrix} \tag{79}$$

$$\frac{d}{dz} \begin{bmatrix} cQ_f + cQ_{\text{re}}^{(f)} \\ I_f + I_{\text{re}}^{(f)} \end{bmatrix} = \begin{bmatrix} 0 & -jk \\ -jk & 0 \end{bmatrix} \begin{bmatrix} cQ_f + cQ_{\text{re}}^{(f)} \\ I_f + I_{\text{re}}^{(f)} \end{bmatrix}$$
$$+ \begin{bmatrix} \displaystyle\sum_m \frac{j\chi(k_m)}{Z_0} \hat{Z}_f(k_m) I_f(0) e^{-jk_m z} \\ 0 \end{bmatrix} - \begin{bmatrix} \displaystyle\sum_m \frac{j\chi(k_m)}{Z_0} \sum_n \hat{Z}_n(k_m) \hat{I}_{\text{re}}^{(f)}(k_n) e^{-jk_m z} \\ 0 \end{bmatrix} \tag{80}$$

$$\frac{d}{dz} \begin{bmatrix} cQ_b + cQ_{\text{re}}^{(b)} \\ I_b + I_{\text{re}}^{(b)} \end{bmatrix} = \begin{bmatrix} 0 & -jk \\ -jk & 0 \end{bmatrix} \begin{bmatrix} cQ_b + cQ_{\text{re}}^{(b)} \\ I_b + I_{\text{re}}^{(b)} \end{bmatrix}$$
$$+ \begin{bmatrix} \displaystyle\sum_m \frac{j\chi(k_m)}{Z_0} \hat{Z}_b(k_m) I_b(L) e^{-jk_m z} \\ 0 \end{bmatrix} - \begin{bmatrix} \displaystyle\sum_m \frac{j\chi(k_m)}{Z_0} \sum_n \hat{Z}_n(k_m) \hat{I}_{\text{re}}^{(b)}(k_n) e^{-jk_m z} \\ 0 \end{bmatrix} \tag{81}$$

$$\frac{d}{dz} \begin{bmatrix} cQ \\ I \end{bmatrix} = \begin{bmatrix} 0 & -jk \\ -jk & 0 \end{bmatrix} \begin{bmatrix} cQ \\ I \end{bmatrix} + \begin{bmatrix} \displaystyle\sum_m \frac{j\chi(k_m)}{Z_0} \left\{ \hat{E}_{\text{ex}}(k_m) + \hat{E}_{\text{tr}}(k_m) - \hat{E}_{\text{fin}}(k_m) \right\} e^{-jk_m z} \\ 0 \end{bmatrix}. \tag{84}$$
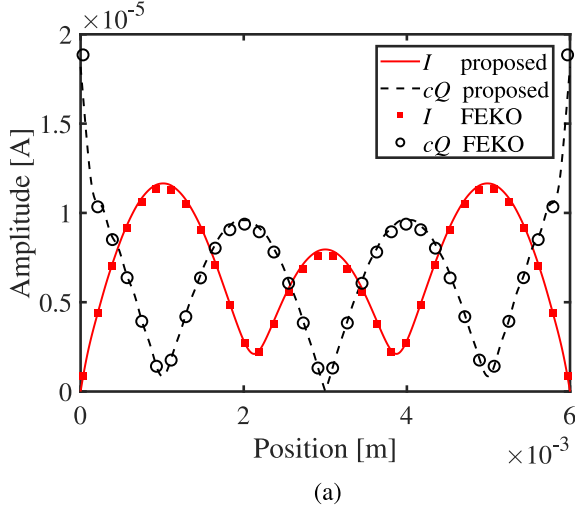
(a)
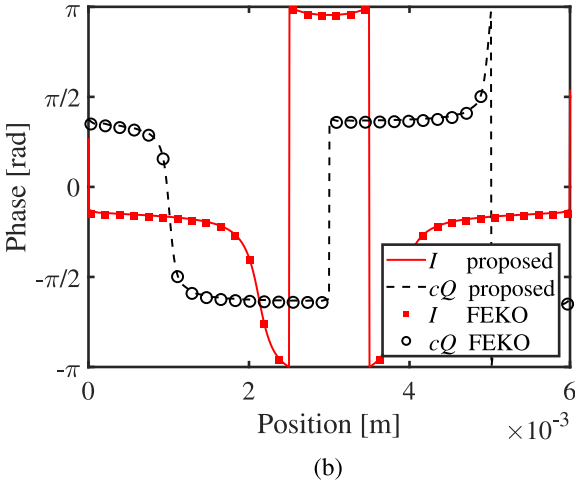


(b)

Fig. 7.    Distribution of total current and charge density ($L = 6$ mm, $a = 15\,\mu$m, $E_{\text{ex}}(z) = 1$ V/m, $f = 75$ GHz). (a) Amplitude. (b) Phase.

The total differential equation for $cQ$ and $I$ can be written as (84) shown at the bottom of this page, by combining (79)–(81), where

$$\hat{E}_{\text{tr}} = \hat{Z}_f(k_m)I_f(0) + \hat{Z}_b(k_m)I_b(L) \tag{85}$$

$$\hat{E}_{\text{fin}} = \sum_n \hat{Z}_n(k_m)\left\{\hat{I}_{\text{sc}}(k_n) + \hat{I}_{\text{re}}(k_n)\right\} \tag{86}$$

denote the electric fields produced by the radiation reaction and finite-length effect, respectively. For the case of an open-circuited wire, the KCL can be applied as a terminal condition at $z = 0$ and $z = L$ to obtain

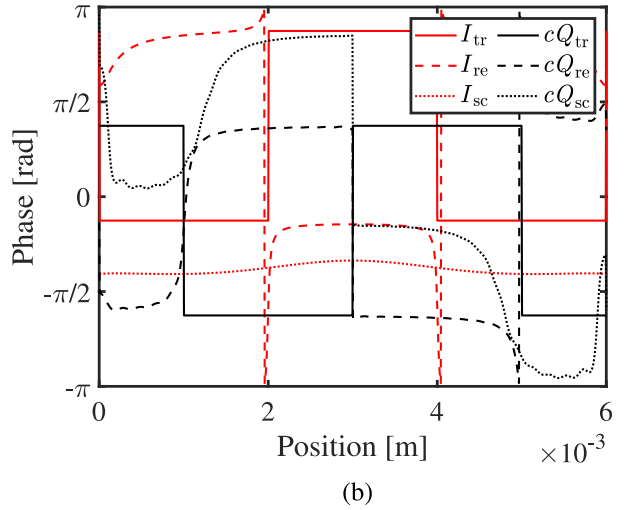$$I_{\text{tr}}(0) + I_{\text{re}}(0) + I_{\text{sc}}(0) = 0 \tag{87}$$

$$I_{\text{tr}}(L) + I_{\text{re}}(L) + I_{\text{sc}}(L) = 0. \tag{88}$$

From these conditions, we obtain the simultaneous equations for $I_f(0)$ and $I_b(L)$ as

$$\begin{bmatrix} 1 + \alpha_{\text{re}}^{(f)}(0) & e^{-jkL} + \alpha_{\text{re}}^{(b)}(0) \\ e^{-jkL} + \alpha_{\text{re}}^{(f)}(L) & 1 + \alpha_{\text{re}}^{(b)}(L) \end{bmatrix} \begin{bmatrix} I_f(0) \\ I_b(L) \end{bmatrix} = \begin{bmatrix} -I_{\text{sc}}(0) \\ -I_{\text{sc}}(L) \end{bmatrix}. \tag{89}$$
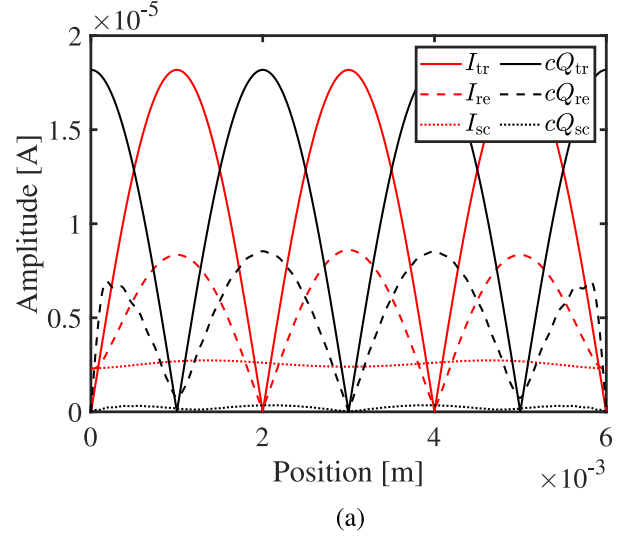


(a)



(b)

Fig. 8.    Distributions of the three components: traveling (tr) wave, radiation reaction (re), and scattering (sc) wave. The conditions are the same as in Fig. 7. These are the component-wise expressions of Fig. 7, the traveling wave becomes the standing wave, the radiation reaction is 180° out of phase with the traveling wave and severely distorted at the wire-ends because of the strong weighting property of the electric field from the traveling wave [see (85)], and the scattering component distributes in accordance with the incident EM field. (a) Amplitude. (b) Phase.

[cf. (29) for an approach that does not consider the finite-length effect and radiation reaction.]

## VI. VALIDATION AND GAINED PHYSICAL INSIGHTS

### A. Validation of the Proposed Model

Here, the proposed formulation is validated through the use of several numerical examples. Fig. 6 shows the radiation reaction characteristics obtained for a wire with the physical and frequency characteristics shown in Fig. 4, with both the finite-length effect and radiation reaction incorporated. The characteristics of the proposed model over a frequency range of 0–200 GHz (covering up to four wavelengths) closely agree with those provided by the MoM approach. In the regions around the resonant frequencies, at which the current diverges in the model without a radiation reaction component [green dashed
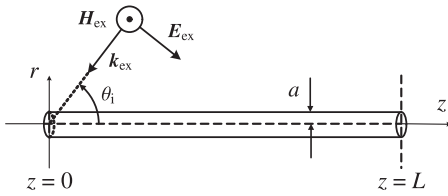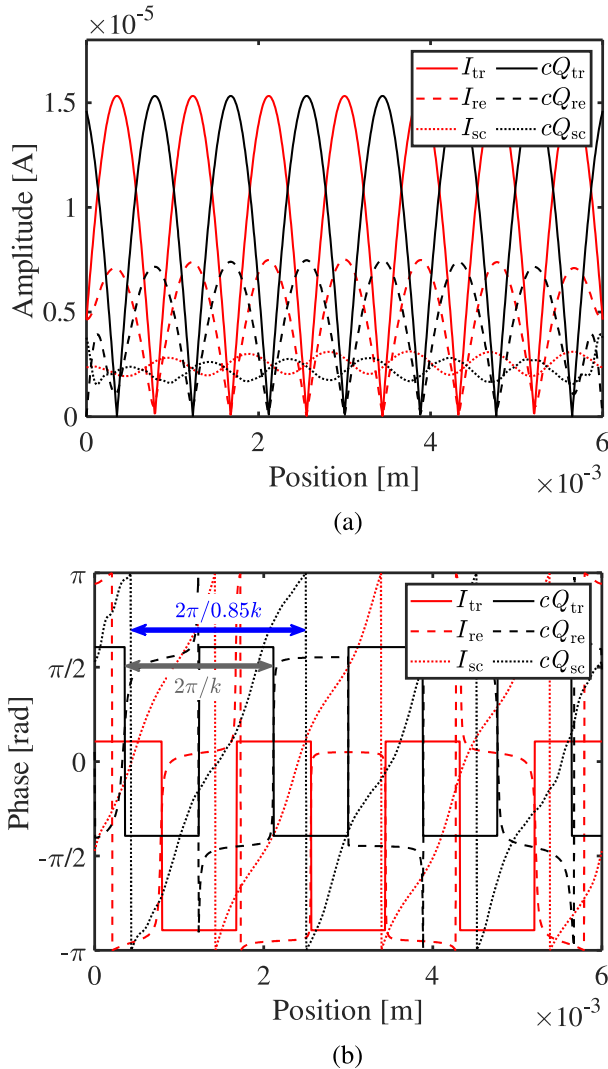
Fig. 9.    Geometry of analytical model.



(a)



(b)

Fig. 10.    Distributions of the three components when a wire with $L = 6$ mm and $a = 15$ $\mu$m is excited by an external plane wave with $|\boldsymbol{E}_{\mathrm{ex}}| = 1$ V/m and $f = 170$ GHz at an oblique incident angle of $\theta_i = 30°$. The distribution of the scattering wave component corresponds to the periodicity caused by the incident plane wave. (a) Amplitude. (b) Phase.

line in Fig. 6, (30)], as described in Section II, the improved model suppresses the current by taking the radiation reaction into account.

We next examine the distributions of $cQ(z)$ and $I(z)$ along the line. As shown in Fig. 7, the frequency of excitation, $f = 75$ GHz (vertical red line in Fig. 6), and the distribution

produced by the proposed model based on (82) and (83) are in close agreement with the results calculated using MoM.

### B. Physical Insights Revealed by the Method

In this section, physical insights are gained through the physical components classified in Fig. 5. For the configuration shown in Fig. 7, the components of traveling wave [see (12)], radiation reaction [see (71) and (72)], and scattering [see (52)] are plotted in Fig. 8. The traveling wave propagates at the speed of light without distortion as in (12), and therefore, its distribution becomes the standing wave in the sinusoidal steady state. Its p.u.l. charges $cQ_{\mathrm{tr}}$ and currents $I_{\mathrm{tr}}$ behave analogously to the relation between line voltages and currents in the classical TL model. In comparison to the traveling wave, the radiation reaction component has approximately half the amplitude [see Fig. 8(a)], and its phase is shifted by 180° [see Fig. 8(b)]. In this way, the model explicitly includes the losses caused by the traveling wave's radiation as the radiation reaction component. The scattering component, the characteristics of which originate from the particular solution for the case of the infinite-length wire [see (15)], is distributed nearly independent of the position $z$. This is in accordance with a wire that is excited in phase by a plane EM wave, reflecting an instantaneous scattering process, which is fundamentally different from the traveling and reaction components that express TL dynamics (for a better understanding, compare Figs. 8–10, which treats the oblique incidence of a plane wave). In the presented theory, open-circuit configuration does not generally indicate that the traveling wave current becomes zero at the wire end (as it does in the classical TL case) because the three components in Fig. 5 comprise a complete model. For the example case of Fig. 8, the condition is $L = 3\lambda/2$, and the traveling wave becomes zero at the wire ends.

Fig. 7(a) shows that the total p.u.l. charges are locally enhanced at both wire ends. This phenomenon corresponds to the radiation reaction component suffering severe distortion in the vicinity of the wire ends in Fig. 8(a). This originates from only the characteristics of electric field components [see (56) and (57)] that induce reaction currents. These field components have strong weighting properties, with each term proportional to the *bare* Green's functions [see (58) and (59)], and these cause distortions in the $z$-distribution, especially around the wire ends.

To confirm that the presented physical components successfully reproduce the actual phenomena, another configuration is tested for a more general case, in which the incident angle of the exciting plane wave becomes oblique ($\theta_i = 30°$ in Fig. 9), and the exciting frequency is out of resonance ($L = 6$ mm, $f = 170$ GHz). The general characteristics of the traveling and reaction components are basically the same as those of Fig. 8, except that $I_{\mathrm{tr}}$ does not become zero at both wire ends because the wire length $L$ is not the integer multiple of a half wavelength here. The scattering component ($cQ_{\mathrm{sc}}$, $I_{\mathrm{sc}}$), the original characteristics of which follow (15), is distributed according to the $z$-directional component of the incident angular wavenumber $k_z = -k \cos 30° = -0.87k$. The $z$-directional angular wavenumber of the scattering component calculated, for instance, from the spatial period of the distribution of $cQ_{\mathrm{sc}}$
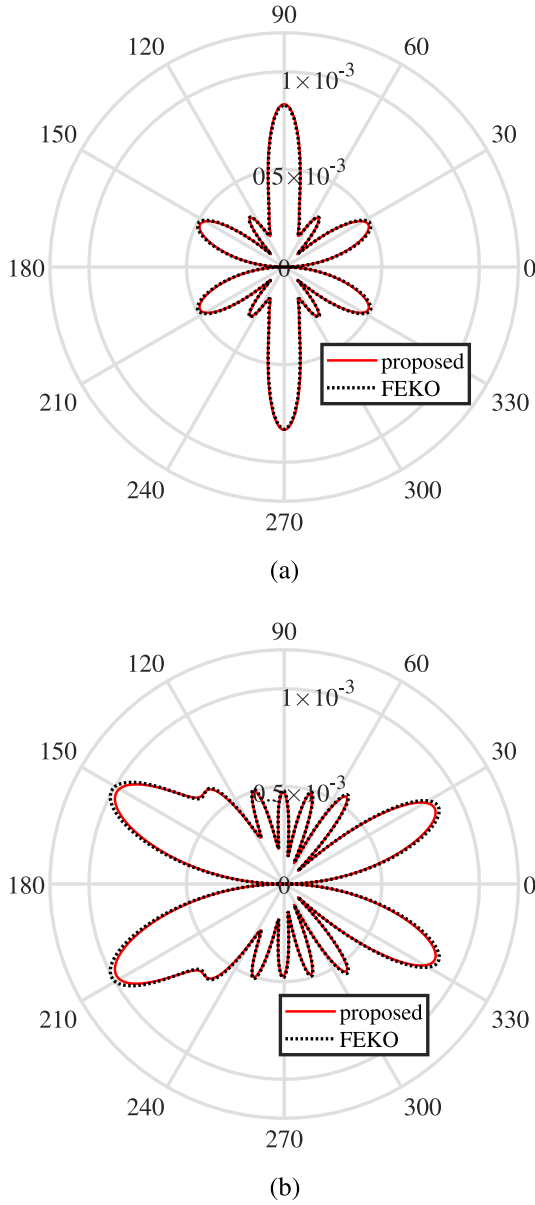
Fig. 11. Radiation patterns for $L = 6$ mm, $a = 15\,\mu$m, $E_{\mathrm{ex}}(z) = 1$ V/m, and $f = 170$ GHz. (a) In-phase excitation, $\theta_i = 90°$ (total). (b) Oblique incidence with $\theta_i = 30°$. The configuration for case (b) corresponds to that in Fig. 10.
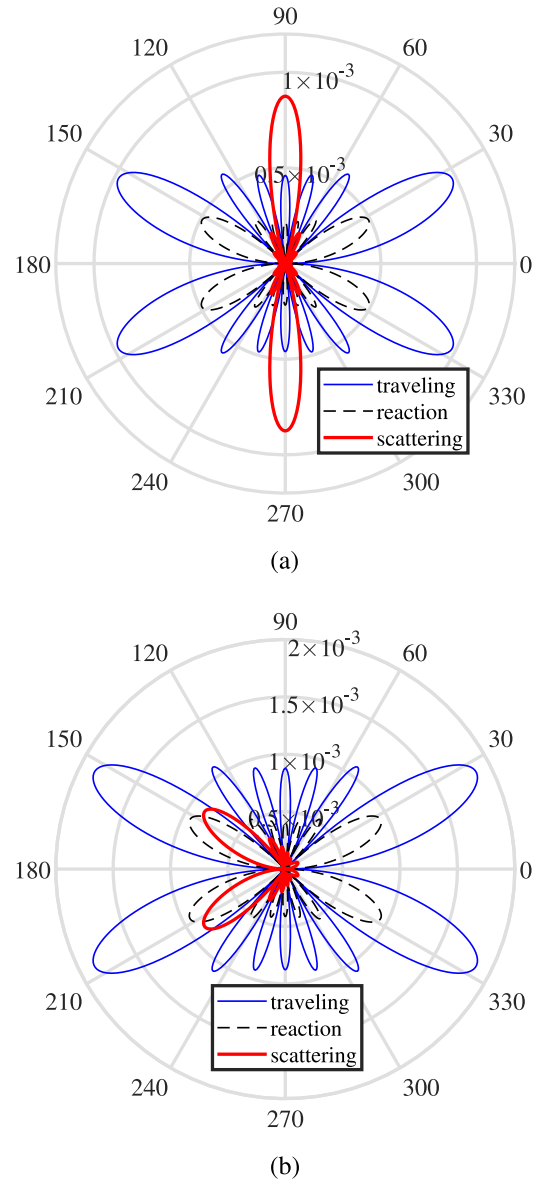
Fig. 12. Component-wise expressions of Fig. 11. The radiation patterns of the traveling and radiation reaction components show the characteristics inherent to the structure (determined by the wire length and frequency). Therefore, they are consistent with Fig. 11(a) and (b). In contrast, the directivity of the scattering component depends heavily on the angle of reflection. (a) $\theta_i = 90°$ (components). (b) $\theta_i = 30°$ (components).

indicated by the blue arrow in Fig. 10(b) becomes $-0.85k$ (for reference, those for traveling and reaction components become $\pm k$ because they propagate at the speed of light). Even in the condition in which whole wavelengths do not comfortably fit into the length of the wire, as in this example, the model is found to consistently reproduce these physical characteristics.

To gain physical insights into the proposed model from the perspective of EM field radiation phenomena, we characterize the far field pattern of the electric field for each component (traveling wave, radiation reaction, and scattering source).

Using Fig. 9 for the test setup, the overall characteristics of the radiation patterns produced by the proposed model and the MoM are compared in Fig. 11. The respective models are in close agreement in terms of both magnitude and directivity. In Fig. 12,

the total radiation pattern produced by the proposed model (the red solid line in Fig. 11) is comprised of the patterns produced by the traveling wave (thin blue line), radiation reaction (black dashed line), and scattering source (red thick line).

Here the characteristics of these three components are explained through invoking the traveling wave antenna theory [34]. The far electric field pattern $|E_\theta|$, produced by the uniform traveling wave element at a single-phase velocity $pc$ [e.g., $p$ adopts the values of 1 and $-1$ for the traveling wave in (13) and (14), respectively], can be expressed as

$$|E_\theta| \propto \left| \frac{kL}{2} \sin\theta \mathrm{sinc}\left\{ \frac{kL}{2}\left( \frac{1}{p} - \cos\theta \right) \right\} \right| \quad (90)$$

where $\text{sinc } x = \sin x/x$, $\theta$ is the polar angle of the observation point, and physical quantities that do not affect the far field pattern are omitted [34]. Equation (90) indicates that the far-field pattern is determined by the phase velocity and wire length. It also indicates that the maximum directivities produced for the forward traveling wave ($p = 1$) are in the directions of $\theta = 27°$ and $333°$, and those for the backward traveling wave ($p = -1$) are in $\theta = 153°$ and $207°$. These reproduce the main lobes of the traveling wave component in both Fig. 12(a) and (b), and the radiation pattern produced by a traveling wave element is independent of the incidence angle $\theta_i$. This is also true for the radiation reaction, which is characterized solely by the traveling wave. Compared to the traveling wave, the far field produced by the radiation reaction component has half the amplitude and a phase difference of $180°$, which is the same as the distribution of source components using Fig. 8. The field produced by the scattering component ($cQ_{\text{sc}}$, $I_{\text{sc}}$) has an approximate directivity corresponding to the angle of reflection of the incident angle $\theta_i$. The reason is explained by (90): *if we suppose that* the source distribution of the scattering component corresponds in periodicity to that of the incident field $E_{\text{ex}}$ (i.e., $k_z = -k\cos\theta_i \sim k/p$ as is discussed using Fig. 10), then the dependence of $\theta$ and $\theta_i$ can be expressed as

$$|E_\theta|(\theta, \ \theta_i) \propto \left| \sin\theta \, \text{sinc} \left\{ -\frac{kL}{2} (\cos\theta_i + \cos\theta) \right\} \right| \quad (91)$$

and its maximum directivity is produced at $\theta \sim 180° \pm \theta_i$. These characteristics closely reflect the physical properties of the traveling wave, radiation reaction, and scattering source.

## VII. Conclusion

In this article, a single-conductor TL model was developed by deriving a homogeneous TL equation for an infinite single conductor, the solution to which corresponds to the Sommerfeld principal wave. Based on the application of classical EM field scattering theory, the effect of the external field is included in the inhomogeneous term of the TL equation. Through this formulation, the circuit constants of the TL equation become independent of position, thereby retaining the dynamics of the principal wave, allowing the propagation and scattering phenomena to be characterized in a simple manner. By considering the effects produced by a wire of finite length, the scattering phenomena can be theoretically extended to the case of a wire with finite length. As the radiation effect is included in the formulation explicitly, the model is beneficial for a better understanding of radiation phenomena that disrupt TL performance. In the proposed model, the current along a wire can be classified into a traveling wave (the principal wave), radiation reaction, and the external field-induced scattering components, all of which associate with the actual phenomena in a simple manner. This significant advantage is obtained along with structural simplification of the fundamental component of the presented theory (i.e., a thin and straight wire).

Our computational results reveal that it will be possible to further simplify the model to facilitate its use, a goal toward which the authors' group is currently working. In addition, the model is potentially more generally applicable to other lumped and distributed constant circuit elements and excitation forms other than a plane EM wave. Potential applications of the model include circuit-based design and synthesis of three-dimensional entangled EM phenomena in a network comprised of straight single-conductor lines. Such a structure could also be analyzed within the framework of the presented TL theory, using the single-wire model as a fundamental building block. These extensions will afford new aspects in studies on topics such as metamaterials, plasmonics, and EMC, where predominant numerical methods are inadequate in terms of interpreting the results owing to a lack of physical insights.

## References

[1] C. R. Paul, *Analysis of Multiconductor Transmission Lines*. New York, NY, USA: Wiley-Interscience, 1994.

[2] F. M. Tesche, M. V. Ianoz, and T. Karlsson, *EMC Analysis Methods and Computational Models*. New York, NY, USA: Wiley, 1997.

[3] J. Nitsch, F. Gronwald, and G. Wollenberg, *Radiating Nonuniform Transmission-Line Systems and the Partial Element Equivalent Circuit Method*. Chichester, U.K.: Wiley, 2009.

[4] P. Besnier, S. Chabane, and M. Klingler, "Some limiting aspects of transmission line theory and possible improvements," *IEEE Electromagn. Compat. Mag.*, vol. 3, no. 2, pp. 66–75, Apr./May 2014.

[5] S. Tkachenko, F. Rachidi, and M. Ianoz, "Electromagnetic field coupling to a line of finite length: Theory and fast iterative solutions in frequency and time domains," *IEEE Trans. Electromagn. Compat.*, vol. 37, no. 4, pp. 509–518, Nov. 1995.

[6] H. Haase, T. Steinmetz, and J. Nitsch, "New propagation models for electromagnetic waves along uniform and nonuniform cables," *IEEE Trans. Electromagn. Compat.*, vol. 46, no. 3, pp. 345–352, Aug. 2004.

[7] D. Poljac, A. Shoory, F. Rachidi, S. Antonijevic, and S. V. Tkachenko, "Time-domain generalized telegrapher's equations for the electromagnetic field coupling to finite length wires above a lossy ground," *IEEE Trans. Electromagn. Compat.*, vol. 54, no. 1, pp. 218–224, Feb. 2012.

[8] H. Toki and K. Sato, "Multiconductor transmission-line theory with electromagnetic radiation," *J. Phys. Soc. Jpn.*, vol. 81, no. 1, pp. 014–201, 2012.

[9] A. Maffucci, G. Miano, and F. Villone, "An enhanced transmission line model for conducting wires," *IEEE Trans. Electromagn. Compat.*, vol. 46, no. 4, pp. 512–528, Nov. 2004.

[10] S. Chabane, P. Besnier, and M. Kingler, "A modified enhanced transmission line theory applied to multiconductor transmission lines," *IEEE Trans. Electromagn. Compat.*, vol. 59, no. 2, pp. 518–528, Apr. 2017.

[11] L. Solymar and E. Shamonina, *Waves in Metamaterials*. New York, NY, USA: Oxford Univ. Press, 2009.

[12] N. Engheta, "Circuits with light at nanoscales: Optical nanocircuits inspired by metamaterials," *Science*, vol. 317, no. 5845, pp. 1698–1702, Sep. 2007, doi: 10.1126/science.1133268.

[13] K. Ohishi, T. Hisakado, T. Matsushima, and O. Wada, "Equivalent-circuit model with retarded electromagnetic coupling for meta-atoms of wired metallic spheres," *IEICE Trans. Electron.*, vol. E101-C, no. 12, pp. 923–930, Dec. 2018, doi: 10.1587/transele.E101.C.923.

[14] K. Wang and D. M. Mittleman, "Metal wires for terahertz wave guiding," *Nature*, vol. 432, pp. 376–379, Nov. 2004.

[15] T. Akalin, A. Treizebré, and B. Bocquet, "Single-wire transmission lines at terahertz frequencies," *IEEE Trans. Microw. Theory Techn.*, vol. 54, no. 6, pp. 2762–2767, Jun. 2006.

[16] F. Monticone and A. Alu, "Leaky-wave theory, techniques, and applications: from microwave to visible frequencies," in *Proc. IEEE*, vol. 103, no. 5, pp. 793–821, May 2015.

[17] T. –I. Jeon, J. Zhang, and D. Grischkowsky, "THz Sommerfeld wave propagation on a single metal," *Appl. Phys. Lett.*, vol. 86, Apr. 2005, Art. no. 161904.

[18] A. Alu and S. Maslovski, "Power relations and a consistent analytical model for receiving wire antennas," *IEEE Trans. Antennas Propag.*, vol. 58, no. 5, pp. 1436–1448, May 2010.

[19] I. Liberal and R. Ziolkowski, "Analytical and equivalent circuit models to elucidate power balance in scattering problems," *IEEE Trans. Antennas Propag.*, vol. 61, no. 5, pp. 2714–2726, May 2013.

[20] A. Sommerfeld, "Über die fortpflanzung elektrodynamischer wellen l ä ngs eines drahtes," *Annalen der Physik und Chemie*, vol. 67, pp. 233–290, 1899.

[21] G. Goubau, "Single-conductor surface-wave transmission lines," in *Proc. IRE*, vol. 39, no. 6, 1951, pp. 619–624.

[22] Y. Baba and V. A. Rakov, "On the mechanism of attenuation of current waves propagating along a vertical perfectly conducting wire above ground: Application to lightning," *IEEE Trans. Electromagn. Compat.*, vol. 47, no. 3, pp. 521–532, Aug. 2005.

[23] A. Vukicevic, F. Rachidi, M. Rubinstein, and S. V. Tkachenko, "On the evaluation of antenna-mode currents along transmission lines," *IEEE Trans. Electromagn. Compat.*, vol. 48, no. 4, pp. 693–700, Nov. 2006.

[24] K. K. Mei, "Theory of Maxwellian circuits," *Radio Sci. Bull.*, vol. 305, pp. 6–13, Sep. 2003, doi: 10.23919/URSIRSB.2003.7909768.

[25] L. Li, Y. W. Liu, K. K. Mei, and K. W. Leung, "Applications of the Maxwellian circuits to linear wire antennas and scatterers," *IEEE Trans. Antennas Propag.*, vol. 54, no. 10, pp. 2725–2730, Oct. 2006, doi: 10.1109/TAP.2006.882174.

[26] D. Tashiro, T. Hisakado, T. Matsushima, and O. Wada, "Formulation of single-conductor transmission line model with feedback electric fields by terminal discontinuity," in *Proc. Asia-Pacific. Microw. Conf.*, Kyoto, Japan, Nov. 2018, pp. 642–644.

[27] J. A. Stratton, *Electromagnetic Theory*. New York, NY, USA: McGraw-Hill, 1941.

[28] R. F. Harrington, *Time-Harmonic Electromagnetic Fields*. New York, NY, USA: McGraw-Hill, 1993.

[29] J. R. Mentzer, *Scattering and Diffraction of Radio Waves*. New York, NY, USA: Pergamon Press, 1955.

[30] J. B. Nitsch and S. V. Tkachenko, "Complex-valued transmission-line parameters and their relation to the radiation resistance," *IEEE Trans. Electromagn. Compat.*, vol. 46, no. 3, pp. 477–487, Aug. 2004, doi: 10.1109/TEMC.2004.831905.

[31] Y. Kami and R. Sato, "Circuit-concept approach to externally excited transmission lines," *IEEE Trans. Electromagn. Compat.*, vol. EMC-27, no. 4, pp. 177–183, Nov. 1985, doi: 10.1109/TEMC.1985.304288.

[32] G. S. Smith, "Teaching antenna radiation from a time-domain perspective," *Amer. J. Phys.*, vol. 69, no. 3, pp. 288–300, Mar. 2001.

[33] R. Lundholm, R. B. Finn, and W. S. Price, "Calculation of transmission line lightning voltages by field concepts," *AIEE Trans. Power App. Syst.*, vol. 77, pp. 1271–1283, Feb. 1958.

[34] J. D. Kraus, *ANTENNAS*, 2nd ed. New York, NY, USA: McGraw-Hill, 1988.

**Daiki Tashiro** (Member, IEEE) received the B.E. and M.E. degrees in electrical engineering from Kyoto University, Kyoto, Japan, in 2017 and 2019, respectively.

Since 2019, he has been with the Central Research Institute of Electric Power Industry (CRIEPI), Yokosuka, Japan. His current research interests include transient analysis and modeling of electrodynamics.

Mr. Tashiro is a member of the Institute of Electronics, Information and Communication Engineers of Japan (IEICE), and the Institute of Electrical Engineers of Japan (IEEJ).

**Takashi Hisakado** (Member, IEEE) received the B.E. and M.E. degrees in electrical engineering II and the Dr. Eng. degree in electrical engineering from Kyoto University, Kyoto, Japan, in 1993, 1995, and 1997, respectively.

He is currently an Associate Professor with the Department of Electrical Engineering, Kyoto University. His research interests include the design of electromagnetic phenomena and power flows.

Dr. Hisakado is a member of the Institute of Electronics, Information and Communication Engineers of Japan, and the Institute of Electrical Engineers of Japan.

**Tohlu Matsushima** (Member, IEEE) received the M.E. and Ph.D. degrees in communication network engineering from Okayama University, Okayama, Japan, in 2006 and 2009, respectively.

From 2009 to 2018, he was an Assistant Professor with the Department of Electrical Engineering, Kyoto University, Kyoto, Japan. He is currently an Associate Professor with the Kyushu Institute of Technology, Kitakyushu, Japan. His research interest is problems with electromagnetic interference.

He is a member of the Institute of Electronics, Information and Communication Engineers of Japan (IEICE), the Institute of Electrical Engineers of Japan (IEEJ), and the Japan Institute of Electronics Packaging (JIEP).

**Osami Wada** (Member, IEEE) received the B.E., M.E., and Dr. Eng. degrees in electronics from Kyoto University, Kyoto, Japan, in 1981, 1983, and 1987, respectively.

From 1988 to 2005, he was with the Faculty of Engineering, Okayama University, Okayama, Japan. In 2005, he became a Full Professor with the Department of Electrical Engineering, Kyoto University. He has been engaged in the study of the electromagnetic compatibility (EMC) of Electronic Circuits and Systems and the development of EMC macro models of integrated circuits.

Prof. Wada was the Chair of IEEE EMC Society Japan Chapter from 2012 to 2013, and the Chair or the Technical Committee of EMC (EMCJ) in the Institute of Electronics, Information and Communication Engineers of Japan (IEICE) from 2017 to 2018. He is a Fellow of IEICE, a member of the Institute of Electrical Engineers of Japan (IEEJ), and the Japan Institute of Electronics Packaging (JIEP).